

Magnetic vacancy percolation in dilute antiferromagnets

W. C. Barber, F. Ye, and D. P. Belanger

Department of Physics, University of California, Santa Cruz, California 95064, USA

J. A. Fernandez-Baca

Condensed Matter Sciences Division, Oak Ridge National Laboratory, Oak Ridge, Tennessee 37831, USA

(Received 17 December 2002; revised manuscript received 27 August 2003; published 21 January 2004)

Neutron-scattering experiments at the magnetic vacancy percolation threshold concentration x_v , using the random-field Ising crystal $\text{Fe}_{0.76}\text{Zn}_{0.24}\text{F}_2$, show stability of the transition to long-range order up to fields $H = 6.5$ T. The observation of the stable long-range order corroborates the sharp boundary observed in computer simulations at x_v separating equilibrium critical scattering behavior at high magnetic concentration from low concentration hysteretic behavior. Low-temperature $H > 0$ scattering line shapes exhibit the dependence on the scattering wave vector expected for percolation threshold fractal structures.

DOI: 10.1103/PhysRevB.69.024409

PACS number(s): 75.40.-s, 25.40.Dn

The dilute, anisotropic antiferromagnet $\text{Fe}_x\text{Zn}_{1-x}\text{F}_2$ is an extensively studied prototype of the three-dimensional ($d = 3$) random-field Ising model (RFIM).¹ As a result of the magnetic vacancies, the magnetic moment is not uniform and this allows a strong coupling to an external magnetic field applied along the spin-ordering direction. This constitutes the mechanism for the generation of random fields.² It was shown that such a system is in the same universality class as a pure Ising magnet with random fields imposed.³ Settling the question of universality of the phase transition does not, however, address the effect of vacancies on microscopic domain formation, which can mask the phase transition in scattering experiments. Such microdomain formation, which occurs since domain walls can take advantage energetically of the vacancies, needs to be well understood in order to properly interpret the RFIM behavior of dilute magnets.

For many years controversy surrounded the interpretation of neutron-scattering experiments¹ on the RFIM critical behavior of dilute anisotropic antiferromagnets in external magnetic fields H , particularly, $\text{Fe}_x\text{Zn}_{1-x}\text{F}_2$ and its less anisotropic isomorph $\text{Mn}_x\text{Zn}_{1-x}\text{F}_2$. All of these studies, regardless of whether traditional scaling or various phenomenological models were used in the interpretations, were done at concentrations $x \leq 0.75$.^{4,5} This was natural since the strength of the random field increases with dilution and available field strengths required high vacancy concentrations to readily create suitably strong random fields. It was, of course, realized that no ordering would take place for magnetic concentration below the magnetic percolation threshold concentration $x_p = 0.246$. The magnetic vacancy percolation threshold concentration occurs at $x_v = 1 - x_p = 0.754$. Below this concentration, vacancies form a cluster that spans the crystal. The significant role of magnetic vacancy percolation in the formation of microdomains was not fully appreciated until recently⁶ and, prior to that, it was widely assumed that microdomain formation was an intrinsic property of the RFIM as realized in dilute antiferromagnets. The microdomain structures for small x have been studied extensively.^{7,8} It has recently been argued that these structures play a crucial role in exchange-bias structures important to magnetic recording technology.^{9,10} Microscopic do-

main structure, for which the characteristic length scale is small compared to the instrumental resolution, masks the neutron-scattering critical behavior for two reasons. First, the scattering contribution from microscopic domains is superimposed on the scattering from thermal fluctuations, making it futile to separate the two. Second, there is a concomitant decrease in the Bragg scattering, which consequently no longer represents the strength of the RFIM order parameter. This has been particularly frustrating, since characterization of the RFIM transition is important in light of the present disagreements between simulations and experiments.⁶

The critical behavior of $\text{Fe}_{0.93}\text{Zn}_{0.07}\text{F}_2$ using neutron scattering techniques provided evidence¹¹ that microscopic domains could be avoided altogether by doing measurements at high magnetic concentrations, although very high quality crystals and high fields are required. Further experiments have been done using $\text{Fe}_{0.85}\text{Zn}_{0.15}\text{F}_2$ and $\text{Fe}_{0.87}\text{Zn}_{0.13}\text{F}_2$.^{12,13} These experiments are providing the avenue for a complete experimental characterization of the RFIM universal critical behavior. It has become quite clear that the behavior at large x is quite distinct from that at low x which exhibits microdomain structure. Computer simulations⁶ were done to model the behavior of the formation of microdomains and long-range order in $\text{Fe}_x\text{Zn}_{1-x}\text{F}_2$ in an attempt to understand how the behavior crosses from one type of behavior to the other. It is suggested by these simulations that low-temperature metastability and microscopic domain formation vanish abruptly above $x = 0.76$, which closely coincides with the concentration of the magnetic vacancy percolation threshold concentration $x_v = 0.754$. Apparently, the percolating lattice of vacancies results in the instability of long-range order below the transition. In previous experiments, little attention has been paid to the percolation of magnetic vacancies. In light of its importance to the understanding of the RFIM we were motivated to investigate the scattering in $\text{Fe}_{0.76}\text{Zn}_{0.24}\text{F}_2$, which is very close to the critical concentration x_v .

Considerable focus has been given to the study of behavior near the complementary threshold concentration for magnetic percolation $x_p = 1 - x_v$, using neutron scattering, specific heat, linear birefringence, magnetization, and ac

susceptibility techniques.^{14–18} The value $x_p=0.246$ is based on a calculation including only the dominant J_2 interaction.¹⁹ However, for concentrations close to x_p , the system is extremely sensitive to very weak interactions that are insignificant away from x_p . Spin-glass-like behavior at $H=0$ has been well characterized. Even far above x_p , large fields cause a crossover from the low-field microdomain-dominated random-field behavior to the spin-glass-like behavior.^{20–25}

The neutron-scattering experiments were performed at the Oak Ridge National Laboratory High Flux Isotope Reactor using a double-axis spectrometer configuration. The beam was horizontally collimated to 20 min of arc before and after the sample and 48 min of arc before the monochromator. The neutron energy was either 13.7 meV on the HB1 spectrometer or 14.7 meV on the HB1A spectrometer. Neutrons with higher order energies were eliminated using pyrolytic graphite filters. Most of the data were taken with transverse scans about the (100) antiferromagnetic Bragg point [i.e., $Q=(1,q,0)$]. The $\text{Fe}_{0.76}\text{Zn}_{0.24}\text{F}_2$ crystal has an irregular shape approximately $4\times 5\times 10\text{ mm}^3$. It has a resolution limited Bragg peak, but very small secondary peaks appear for $q>0$ in the low-temperature scans, indicating the existence of more than one crystal in the sample. Near the transition, these tiny peaks are not evident. All the data used in the analysis of the line shapes at low temperatures are on the $q<0$ side of the Bragg peak, where no hints of any secondary peaks are observed. The thermometry was based on a commercially calibrated carbon thermometer. However, the thermometry bridge itself was not well calibrated and the temperature scale had to be adjusted so that the transition corresponds to that expected for $x=0.76$. The concentration was determined to be $x=0.76\pm 0.01$ using density measurements and the concentration gradient of a few tenths of a percent was determined using room temperature birefringence techniques.²⁶ An independent determination of the concentration was made by measuring the absolute birefringence of the sample and comparing it to the results of a previous study of the concentration dependence of the birefringence in $\text{Fe}_x\text{Zn}_{1-x}\text{F}_2$ at room temperature.²⁶ We used a 45 deg wedge to measure the critical angle for the two polarizations, a slightly different technique than employed in the previous work. The concentration determined using this technique is $x=0.76\pm 0.02$, consistent with the density measurement. The interpretation of the results were not dependent on this adjustment of the thermometry scale. Two primary thermal cycling procedures that are often employed to investigate hysteresis in the RFIM include: 1) zero-field-cooling (ZFC), where the sample is cooled in the absence of a field, the field is raised, and the sample is warmed through the transition, and 2) field-cooling (FC), where the sample is cooled in the field across the transition.

Figure 1 shows scattering intensity vs q , in reciprocal lattice units (rlu), at $H=3$ and 5 T close to the transition temperatures $T_c=59.3$ and 58.6 K, respectively, where the transition at $H=0$ is at approximately 59.8 K. Whereas the critical scattering from samples with $x<x_v$ exhibits strong hysteresis, it is clear that the $|q|>0$ critical scattering shown

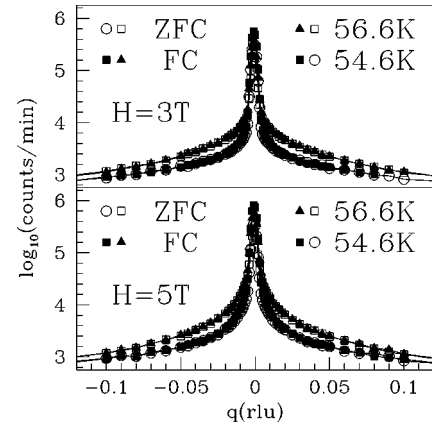


FIG. 1. ZFC and FC neutron scattering at $H=3$ and 5 T below but close to the transition temperature. The contributions include a constant background, critical scattering which is seen to increase as the temperature approaches $T_c(H)$, and a Bragg peak due to long-range order.

in Fig. 1 is free from hysteresis indicating that there is no microscopic domain structure frozen in upon FC.

For experiments free of extinction effects, the magnetic Bragg scattering intensity is expected to follow the power-law behavior

$$I = M_s^2 \sim |t|^{2\beta}, \quad (1)$$

where M_s is the staggered magnetization and $\beta \approx 0.35$ for the random-exchange model and $\beta \approx 0.16$ for the RFIM.¹³ However, neutron scattering in high-quality bulk crystals can suffer from severe extinction; the beam is depleted of neutrons that satisfy the Bragg condition and the scattering intensity is therefore saturated and cannot exhibit the correct T dependence. The extinction effects usually preclude determination of a reliable value of β , the critical exponent for the staggered magnetization, from an analysis of the neutron-scattering data in very high-quality bulk crystals. The Bragg scattering does show hysteresis, which indicates incomplete FC ordering on very long length scales, relative to the instrumental resolution. Such hysteresis occurs for all x , is a clear indication of nonequilibrium behavior, and may be a consequence of the slow activated dynamics^{27–30} of the RFIM very close to $T_c(H)$.

The FC Bragg intensity, corrected for the background determined at high T , is shown in the main part of Fig. 2 vs T for $H=3$ T. The lower inset shows the differing behaviors of ZFC and FC Bragg scattering intensities near $T_c(H)$. The difference persists to low temperatures where critical scattering is very small. Hence, the hysteresis is predominantly from Bragg scattering and not small q critical scattering. The upper inset of Fig. 2 shows the critical scattering at small q , but well outside the transverse instrumental resolution where the Bragg intensity is negligible. The scattering line shapes in this sample are complicated by admixture of critical scattering and contributions from the vacancy lattice because of the proximity of this sample to x_v , as will be discussed. Hence, we could not confidently analyze in detail the critical scattering line shape. Nevertheless, we obtained an approximate accounting of the critical scattering intensity by taking a squared-Lorentzian line shape folded with the appropriate

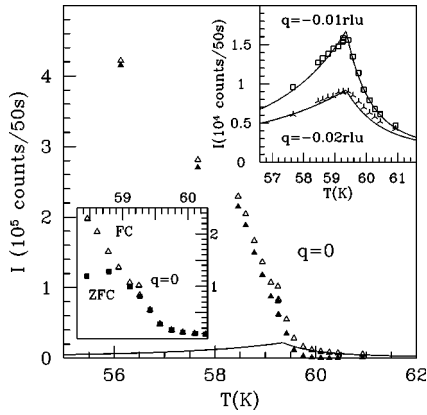


FIG. 2. The ZFC and FC antiferromagnetic Bragg peak intensities for $H=3$ T. In the main figure, the contribution to the FC intensity at $q=0$ due to critical fluctuations is subtracted from the data represented by the open symbols to give the corrected intensities represented by the solid symbols. The upper inset shows the critical scattering off the Bragg peak along with the fit as described in the text. The same fit was used to subtract the critical scattering contribution in the main figure. The lower inset shows the difference between the ZFC and FC intensities. The units for the lower inset are the same as the main figure.

resolution correction. It is well documented that the squared-Lorentzian contribution to the line shape is the dominant one near the transition.¹ An overall amplitude had to be chosen for the fit shown in the inset. This same amplitude was applied to the $q=0$ case and the resulting curve is shown in the main part of Fig. 2 as the solid curves. Subtracting this from the raw data (open symbols) yields the corrected Bragg scattering data (filled symbols). Taking into account the concentration gradient rounding of a few tenths of a percent, it is quite apparent that the Bragg intensity data approach $T_c(H)$ with a steep slope, in contrast with scattering experiments³¹ with $x < x_v$, where the slope is nearly zero.

Although we cannot analyze the data according to Eq. (1) to obtain β because of extinction, we may still conclude from the shape of the Bragg intensity vs T that this sample does not form microscopic domain structure. This is consistent with the lack of hysteresis in the critical scattering shown in Fig. 1. These results suggest that the at least most of the sample has a concentration above the point where domains form at low temperature, a point that simulations indicate to be x_v .

At the percolation threshold concentrations, magnetic sites or magnetic vacancy sites form fractal structures. In either case, scattering from the fractal structure will exhibit a power-law behavior^{32,33}

$$I_f \sim q^{-2.53}. \quad (2)$$

The only difference is that in the case of magnetic vacancies there is also a Bragg scattering peak from the average M_s . With magnetic site percolation, the average M_s is zero at the threshold. Since we believe the $x=0.76$ crystal is close to x_v , we plotted the logarithm of the scattering intensity vs the logarithm of $-q$ for $q < 0$ in Fig. 3. Only some of the scans

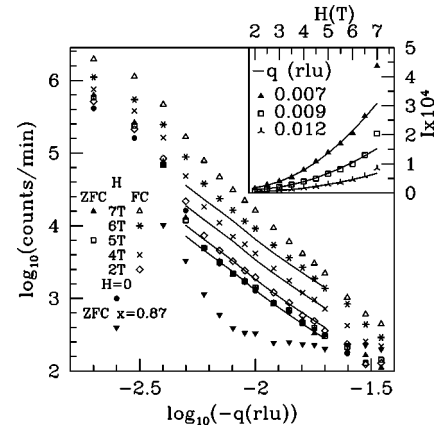


FIG. 3. The logarithm of the neutron-scattering intensity vs the logarithm of q for $H=0$ T and for ZFC at $T=29$ K and FC up to $H=7$ T at $T=20$ K, well below $T_c(H)$. The background determined at large q has been subtracted. Only a few sets of data are shown for clarity. All ZFC data lie on the same curve, but only $H=5$ and 7 T data are shown.

are shown; data were taken for $H=0$ and for $2 \text{ T} < H < 7 \text{ T}$ in steps of 0.5 T . Several interesting features are evident.

As shown explicitly for two fields, $H=5$ and 7 T in Fig. 3, the ZFC line shapes, for $T=29 \text{ K}$ or less, are all identical with the $H=0$ line shape and are the lowest in intensity. For comparison, a line with a fractal exponent of 2.53 for three dimension, with the spectrometer resolution folded in, is plotted in the graph with the amplitude adjusted to fit the ZFC intensity data. It is clear that the ZFC scattering line shapes for $x=0.76$ follow Eq. (2) quite well. To contrast this behavior, we show in Fig. 3 similar data for a sample with concentration of $x \approx 0.87$,¹² indicated by the solid triangles, for $T=55.1 \text{ K}$, only 3.4 K below the transition. The scattering of scattering outside the Bragg region as expected since the vacancies do not form large fractal structures at this concentration. The behavior for ZFC shown in Fig. 3 suggests strongly that, for $x=0.76$, the scattering is indeed from the vacancy percolation fractal structure under the ZFC procedure.

The FC data for $x=0.76$ increase in intensity with the applied field. We compare the data to Eq. (2) by adjusting the amplitude to fit the data at $q = 10^{-1.7} \text{ rlu}$. It is quite clear that for $H > 0$ the line shapes deviate strongly from the behavior in Eq. (2), more so as the field increases. The inset of Fig. 3 shows the deviations of the intensities from the curves representing Eq. (2) at $q = -0.007$, -0.009 , and -0.012 rlu as a function of the applied field. The deviations for $H \leq 6.5 \text{ T}$ increase smoothly with the field. Two possible sources exist for the excess scattering. One is the relief of extinction. This has been observed for neutron Bragg scattering in the RFIM experiments on bulk crystals,¹ but not for scattering outside the Bragg region. The other possibility, perhaps more significant, is the scattering from domains, which coexist with antiferromagnetic long-range order, which increase in number with increasing applied field. If the latter is the case, it can-

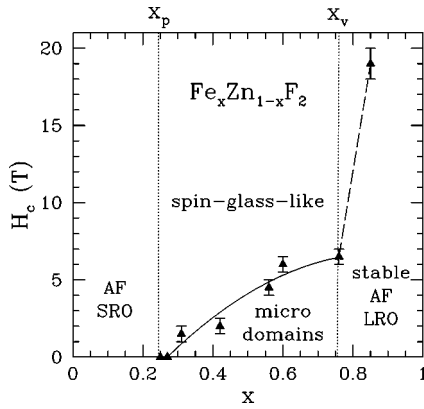


FIG. 4. The concentration dependence of the phases observed in $\text{Fe}_x\text{Zn}_{1-x}\text{F}_2$. For $x < x_p$, the magnetic percolation threshold concentration, only antiferromagnetic short-range order is possible. For $x_p < x < x_v$, microscopic domain formation occurs at low fields and spin-glass-like behavior occurs at high fields. For $x > x_v$, antiferromagnetic long-range order is stable, without microscopic domain formation, to very large applied fields. Critical behavior measurements can only be reliably done for $x > x_v$. Data are taken from various experiments cited in the text.

not be ruled out that the domains are in fact in a part of the sample that is below the critical concentration, although such a part would necessarily be very small since the effects of it are not discernible near $T_c(H)$. Since the total scattering in FC comes from sources in addition to that of vacancy sites, it is difficult to analyze in detail.

The difference between FC intensities and Eq. (2) at $H = 7$ T deviate strongly from the smooth curves describing the data for $H \leq 6.5$ T, as shown in the inset of Fig. 3. This qualitatively new behavior most likely represents a breakdown of the antiferromagnetic long-range structure for $H > 6.5$ T. In such a case many more domains are introduced into the system, resulting in much more scattering intensity. This field is consistent with the increasing field at which spin-glass-like behavior appears for samples with $x < x_v$, as shown in Fig. 4. Apparently, even at low-temperatures, long-range antiferromagnetic order for $x = 0.76$ is stable upon FC for $H < 7$ T, in contrast to the behavior for $x < x_v$, where metastable domains dominate the scattering under the FC procedure. For $x \approx 0.87$, only a few percent above x_v , magnetization experiments³⁴ indicate that the transition to long-range antiferromagnetic order breaks down only for fields above $H = 18$ T, nearly three times the field that causes a breakdown in the behavior of the sample with $x = 0.76$, demonstrating the stability of antiferromagnetic order for $x > x_v$.

We have shown that the magnetic concentration range for which equilibrium random-field critical scattering is observed for dilute antiferromagnets in an external field has a

lower bound at x_v . Whereas our $x = 0.76$ crystal shows no critical scattering hysteresis, it is quite evident for slightly smaller magnetic concentrations.⁵ Our results suggest that the percolation of vacancy sites occurring for $x < x_v$ precipitates the formation of domains below $T_c(H)$ in ZFC preparation as well as in FC, corroborating the conclusions drawn from simulations.⁶ A connection between the one dimensional fractal geometry of vacancy sites at percolation and three dimensional domains has not been adequately explained from a theoretical perspective.

It is now evident that there are three magnetic concentration regimes in $d = 3$ dilute antiferromagnets separated by the percolation threshold concentrations x_p and x_v . For $x > x_v$, long-range antiferromagnetic order is stable up to very large magnetic fields. For $x_p < x < x_v$ the system is unstable. At low fields, the formation of microdomain structure takes place upon FC for all $T < T_c(H)$ and upon ZFC close to $T_c(H)$. A spin-glass-like phase forms at high field. Below x_p , there can be no long-range magnetic order. It is the geometry of the lattice in question which defines the location of these boundaries, and although we study one particular magnetic lattice type, the body-centered tetragonal structure of $\text{Fe}_x\text{Zn}_{1-x}\text{F}_2$, our results should apply more generally to dilute magnets in an applied field.

Interestingly, the specific-heat behavior is not dependent in an obvious way on the concentration. Similar hysteresis upon FC and ZFC is observed¹ very close to $T_c(H)$ for concentrations above and below x_v . No specific-heat hysteresis is observed at low T . The contrast between the relative insensitivity of the specific-heat techniques with the extreme sensitivity of the scattering techniques is certainly due to the greater dependence of the scattering on long length correlations that are greatly affected by domain formation. The hysteresis in the case of specific heat is related to the activated dynamics very close to $T_c(H)$ that affects the behavior at all x and not domain formation, which only occurs for $x < x_v$.

From the results of this investigation, we conclude that studies of the random-field phase transition should be conducted with magnetic concentrations greater than x_v . It is advantageous to use concentrations not too much greater than this to maximize the random fields for available applied fields. However, if the concentration is too close to x_v , one must take into account scattering from the magnetic vacancy percolation cluster. Recent experiments at $x = 0.87$ indicate that, at this concentration, such scattering is negligible.^{12,13}

We thank Stephanie Meyer and Leslie Shelton for assisting in the determination of the concentration of the sample. This work was funded by U.S. Department of Energy Grant No. DE-FG03-87ER45324 and by the Oak Ridge National Laboratory, which is managed by UT-Battelle, LLC, for the U.S. Department of Energy under Contract No. DE-AC05-00OR22725.

¹D.P. Belanger, Braz. J. Phys. **30**, 682 (2000); D.P. Belanger, in *Spin Glasses and Random Fields*, edited by A.P. Young (World Scientific, Singapore, 1998), and references therein.

²S. Fishman and A. Aharony, J. Phys. C **12**, L729 (1979).

³J.L. Cardy, Phys. Rev. B **29**, 505 (1984).

⁴D.P. Belanger, S.M. Rezende, A.R. King, and V. Jaccarino, J. Appl. Phys. **57**, 3294 (1985).

⁵J.P. Hill, Q. Feng, R.J. Birgeneau, and T.R. Thurston, Phys. Rev.

- Lett. **70**, 3655 (1993), although the nominal concentration is $x = 0.75$ the actual concentration may be slightly less, judging from the $H=0$ transition temperature (Ref. 35).
- ⁶W.C. Barber and D.P. Belanger, J. Appl. Phys. **87**, 7049 (2000).
 - ⁷S.-J. Han, D.P. Belanger, W. Kleemann, and U. Nowak, Phys. Rev. B **45**, 9728 (1992).
 - ⁸D.P. Belanger, V. Jaccarino, A.R. King, and R.M. Nicklow, Phys. Rev. Lett. **59**, 930 (1987).
 - ⁹P. Miltnyi, M. Gierlings, J. Keller, B. Beschoten, G. Guntherodt, U. Nowak, and K.D. Usadel, Phys. Rev. Lett. **84**, 4224 (2000).
 - ¹⁰S. Zhang, D.V. Dimitrov, G.C. Hadjipanayis, J.W. Cai, and C.L. Chien, J. Magn. Magn. Mater. **198-199**, 468 (1999).
 - ¹¹Z. Slanic, D.P. Belanger, and J.A. Fernandez-Baca, Phys. Rev. Lett. **82**, 426 (1999).
 - ¹²F. Ye, M. Matsuda, S. Katano, H. Yoshizawa, J.A. Fernandez-Baca, and D. P. Belanger (unpublished).
 - ¹³F. Ye, L. Zhou, S. Laroche, L. Lu, D.P. Belanger, M. Greven, and D. Lederman, Phys. Rev. Lett. **89**, 157202 (2002).
 - ¹⁴D.P. Belanger and H. Yoshizawa, Phys. Rev. B **47**, 5051 (1993).
 - ¹⁵F.C. Montenegro, M.D. Coutinho-Filho, and S.M. Rezende, Europhys. Lett. **8**, 382 (1989).
 - ¹⁶E.P. Barbosa, E.P. Raposo, and M.D. Coutinho-Filho, J. Appl. Phys. **87**, 6531 (2000).
 - ¹⁷W.C. Barber and D.P. Belanger, Phys. Rev. B **61**, 8960 (2000).
 - ¹⁸K. Jonason, C. Djurberg, P. Nordblad, and D.P. Belanger, Phys. Rev. B **56**, 5404 (1997).
 - ¹⁹M.F. Sykes and J.W. Essam, Phys. Rev. **133**, A310 (1964).
 - ²⁰F.C. Montenegro, A.R. King, V. Jaccarino, S.-J. Han, and D.P. Belanger, Phys. Rev. B **44**, 2155 (1991).
 - ²¹D.P. Belanger, Wm. E. Murray, Jr., F.C. Montenegro, A.R. King, V. Jaccarino, and R.W. Erwin, Phys. Rev. B **44**, 2161 (1991).
 - ²²F.C. Montenegro, K.A. Lima, M.S. Torikachvili, and A.H. Lacerda, Mater. Sci. Forum **302-303**, 371 (1999).
 - ²³F.C. Montenegro, K.A. Lima, M.S. Torikachvili, and A.H. Lacerda, J. Magn. Magn. Mater. **177-181**, 145 (1998).
 - ²⁴A. Rosales-Rivera, J.M. Ferreira, and F.C. Montenegro, Europhys. Lett. **50**, 264 (2000).
 - ²⁵J. Satooka, H. Aruga Katori, A. Tobo, and K. Katsumata, Phys. Rev. Lett. **81**, 709 (1998).
 - ²⁶A.R. King, I.B. Ferreira, V. Jaccarino, and D.P. Belanger, Phys. Rev. B **37**, 219 (1988).
 - ²⁷D.S. Fisher, Phys. Rev. Lett. **56**, 416 (1986).
 - ²⁸A.R. King, J.A. Mydosh, and V. Jaccarino, Phys. Rev. Lett. **56**, 2525 (1986).
 - ²⁹A.E. Nash, A.R. King, and V. Jaccarino, Phys. Rev. B **43**, 1272 (1991).
 - ³⁰Ch. Binek, S. Kuttler, and W. Kleemann, Phys. Rev. Lett. **75**, 2412 (1995).
 - ³¹D.P. Belanger, J. Wang, Z. Slanic, S.-J. Han, R.M. Nicklow, M. Lui, C.A. Ramos, and D. Lederman, Phys. Rev. B **54**, 3420 (1996).
 - ³²D. Stauffer and A. Aharony, *Introduction to Percolation Theory*, 2nd ed. (Francis and Taylor, London, 1994).
 - ³³H. Ikeda, K. Iwasa, J.A. Fernandez-Baca, and R.M. Nicklow, Physica B **213**, 146 (1995).
 - ³⁴T. Sakon, A. Awaji, M. Motokawa, and D.P. Belanger, J. Phys. Soc. Jpn. **71**, 411 (2002).
 - ³⁵D.P. Belanger, A.R. King, F. Borsa, and V. Jaccarino, J. Magn. Magn. Mater. **15-18**, 807 (1980).